

# Reactions of Odd-Electron Cobaltacycles: Characterization of a Persistent 17-Electron Anionic Intermediate in Electron-Transfer-Catalyzed (ETC) Substitution Reactions

Bernadette T. Donovan-Merkert,<sup>\*,†,‡</sup> Philip H. Rieger,<sup>§</sup> and William E. Geiger<sup>\*,†</sup>

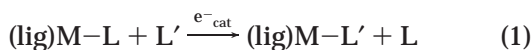
Departments of Chemistry, University of Vermont, Burlington, Vermont 05405, and  
Brown University, Providence, Rhode Island 02912

Received April 7, 1999

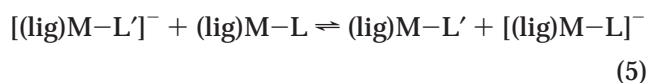
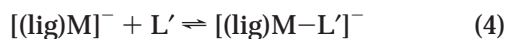
The cobaltfluorene complex  $\text{Cp}(\text{PPh}_3)\text{CoC}_{12}\text{H}_8$  (**1**) undergoes an electrochemically irreversible one-electron reduction in THF ( $E_{p,c} = \text{ca. } -2.56 \text{ V vs ferrocene}$ ) with release of  $\text{PPh}_3$  to give a persistent 17-electron  $\text{Co}(\text{II})$  monoanion,  $\mathbf{2}^-$ , which was characterized by electrochemistry and by ESR spectroscopy. The unpaired spin density in  $\mathbf{2}^-$  is highly delocalized, with the majority being located in the cyclopentadienyl ring rather than the cobaltacyclic fragment. Reoxidation of  $\mathbf{2}^-$  in the presence of L (L = phosphines, phosphites) forms  $\text{Cp}(\text{L})\text{CoC}_{12}\text{H}_8$  in high yield. Slow electron-transfer-catalyzed (ETC) substitution processes are found when **1** is electrolyzed in the presence of  $\text{P}(\text{OMe})_3$ , with the efficiency of the catalysis being dependent on both the relative and absolute concentrations of **1** and  $\text{P}(\text{OMe})_3$ . The substitution reaction is accounted for by a model in which the anion  $\mathbf{2}^-$  is in equilibrium with the 19-electron adducts  $[\text{Cp}(\text{L})\text{CoC}_{12}\text{H}_8]^-$ , where L = THF,  $\text{PPh}_3$ ,  $\text{P}(\text{OMe})_3$ . Further reduction of  $\mathbf{2}^-$  is possible in a reversible one-electron reduction ( $E_{1/2} = -2.80 \text{ V}$ ) to an 18-electron dianion that is stable in solution. The dianion  $\mathbf{2}^{2-}$  was characterized by  $^1\text{H}$  NMR spectroscopy and shown to have  $C_s$  or higher symmetry.

## Introduction

Electron-transfer catalysis (ETC) may provide a mild and therefore preferable route for ligand substitution processes of organometallic compounds.<sup>1–5</sup> Reductively induced ETC reactions (eq 1) implicitly involve a dis-



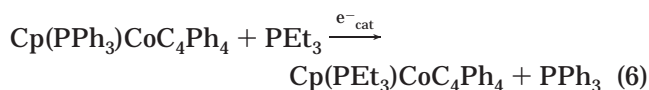
sociative mechanism (eqs 2–5) in which a key intermediate is an electron-deficient complex.<sup>6</sup> In the catalytic



cycle given by eqs 2–5, typical of that expected for a mononuclear complex, this intermediate appears as  $[(\text{lig})\text{M}]^-$  in one of the propagation steps (eq 3). The

equilibria of eqs 3 and 4 involving conversions between 17-electron and 19-electron systems are in general difficult to characterize owing to the high inherent reactivities and lack of NMR properties of the odd-electron species.

When characterizing an electrode-catalyzed substitution of  $\text{PEt}_3$  for  $\text{PPh}_3$  in cobaltacycle **4** (eq 6), we postulated the intermediacy of the 17-electron anion  $\mathbf{5}^-$ .<sup>7</sup>



Although the observed ETC chemistry argued for reversibility of the proposed dissociation step of eq 7 to be reversible, voltammetric measurements were ambiguous, failing to distinguish between reversible and irreversible loss of  $\text{PPh}_3$  from the 19-electron anion  $\mathbf{4}^-$ .



Characterization of the 17  $e^-$ /19  $e^-$  equilibrium of eq 7 was hampered by the instability of  $\mathbf{5}^-$ , which undergoes protonation and rearrangement to give the  $\pi$ -complex  $\text{CpCo}(\text{tetraphenylbutadiene})$ .<sup>7</sup>

Given the importance of 17  $e^-$ /19  $e^-$  equilibria in odd-electron organometallic reactions,<sup>1,8–10</sup> we judged this

<sup>†</sup> University of Vermont.

<sup>‡</sup> Present address: Department of Chemistry, University of North Carolina at Charlotte, Charlotte, North Carolina 28223.

<sup>§</sup> Brown University.

(1) Astruc, D. *Electron-Transfer and Radical Processes in Transition Metal Chemistry*; VCH: New York, 1995; Chapter 6.

(2) Amatore, C. In *Organometallic Radical Processes*; Trogler, W. C., Ed.; Elsevier: Amsterdam, 1990; pp 31–34.

(3) Coville, N. J. In *Organometallic Radical Processes*; Trogler, W. C., Ed.; Elsevier: Amsterdam, 1990; pp 108–141.

(4) Chanon, M., Juliard, M., Poite, J. C., Eds. *Paramagnetic Species in Activation, Selectivity and Catalysis*; Kluwer: Dordrecht, The Netherlands, 1988.

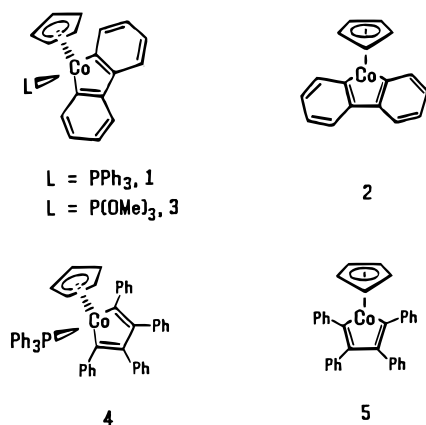
(5) Kochi, J. K. In *Organometallic Radical Processes*; Trogler, W. C., Ed.; Elsevier: Amsterdam, 1990; Chapter 7.

(6) Leading references to postulated structures of unsaturated intermediates in ETC reactions may be found in ref 1, pp 434–445. See also: Poli, R.; Owens, B. E.; Linck, R. G. *J. Am. Chem. Soc.* **1992**, *114*, 1303.

(7) Kelly, R. S.; Geiger, W. E. *Organometallics* **1987**, *6*, 1432.

(8) Kochi, J. K. In ref 5, pp 201–213.

system to be worthy of further study if an intermediate could be found which was not subject to side reactions such as the  $\sigma/\pi$  rearrangement that limited investigations of  $4^-/5^-$ . This paper reports results on an analogue which is indeed impervious to side reactions, at least over about a 1 h time period at ambient temperatures. The 17-electron cobaltafluorenyl anion  $2^-$  generated by one-electron reduction of **1** has been characterized by its electrochemical and ESR spectroscopic properties, by its conversion to 16- and 18-electron systems **2** and  $2^{2-}$ , respectively, and by its ability to take part in ETC substitution reactions. Combination of the ESR results with those of EHMO calculations shows that there is surprisingly little delocalization of the odd electron in  $2^-$  into the fluorenyl ring. A preliminary account of part of this work has appeared.<sup>11</sup>



## Experimental Section

**Preparations. General Considerations.** Synthetic manipulations were carried out using standard Schlenk techniques. The dinitrogen gas was purified with RX-11 copper catalyst (Chemlog), Aquasorb, and activated molecular sieves (t.h.e. Desiccant, EM Science). Solvents were first dried over an appropriate drying agent (Et<sub>2</sub>O, THF, toluene, and hexanes over potassium; CH<sub>2</sub>Cl<sub>2</sub> over calcium hydride) and then distilled immediately prior to use.

CpCo(CO)<sub>2</sub><sup>12</sup> and CpCo(PPh<sub>3</sub>)<sub>2</sub><sup>13</sup> were prepared by the literature procedures, except that with the latter a reaction time of 15 h was used in place of the recommended 3 days. The preparation of 2,2'-dibromobiphenyl also involved a slight modification of the published procedure.<sup>14</sup> Addition of *n*-butyllithium to the solution of *o*-dibromobenzene was conducted at 183 K rather than at 195 K. At the higher temperature, an unidentified brown oil was obtained instead of the desired product. Complex **1** was prepared by the method of Wakatsuki and co-workers.<sup>15</sup>

**Preparation of 3.** The trimethyl phosphite derivative **3** was synthesized by electrochemically reducing a solution of **1** (122.7 mg, 0.228 mmol) in 50 mL of 0.1 M TBAPF<sub>6</sub>/THF at -2.00 V in the presence of P(OMe)<sub>3</sub> (2.78 g, 22.8 mmol, 100 equiv). Although the *i* vs *t* curve indicated completion of the bulk reduction after 8 min, the electrolysis was allowed to

proceed for an additional 4 min to ensure completion of the reaction. Only 0.1 faraday/equiv was required for the electrolysis, which caused the yellow-orange solution to become lighter yellow. Steady-state voltammograms at a rotating platinum electrode showed that greater than 95% conversion to **3** had occurred. Isolation of **3** from the electrolysis solution was achieved by removing most of the THF under reduced pressure, adding 20 mL of Et<sub>2</sub>O, and cooling the mixture to 253 K for 15 min to precipitate most of the supporting electrolyte. After filtration the filtrate was condensed to approximately 3 mL and added under N<sub>2</sub> to a 2.5 × 15 cm chromatography column of activity III neutral alumina. After flushing PPh<sub>3</sub> and P(OMe)<sub>3</sub> through with hexane, the desired complex was eluted with Et<sub>2</sub>O. Removal of ether afforded a fluffy yellow powder identified as **3**. Yield: 48.6 mg (70.5%). Anal. Calcd: C, 60.00; H, 5.55. Found: C, 60.19; H, 5.54. <sup>1</sup>H NMR (CDCl<sub>3</sub>): metallacycle resonances at  $\delta$  7.66 (d, 2H), 7.63 (d, 2H), 7.00 (dd, 2H), 6.83 (dd, 2H), 4.97 (s, 5H, Cp), 3.21 [d, 9H, P(OMe)<sub>3</sub>]. Mass spectrum (CI): parent ion peak at *m/e* 400, base peak at *m/e* 277. Cyclic voltammetry (0.5 mM in 0.1 M THF/[NBu<sub>4</sub>][PF<sub>6</sub>], Pt bead working electrode, SCE reference electrode): irreversible reduction at  $E_{p,c} = -2.76$  V; partially chemically reversible oxidation at  $E_{1/2} = 0.42$  V.

**Electrochemical Methods.** Cyclic voltammetry (CV) experiments were performed using a Princeton Applied Research (PAR) Model 173 potentiostat and a PAR Model 176 current to voltage converter in conjunction with either a PAR 175 universal programmer or a Hewlett-Packard (HP) Model 3300A function generator equipped with a HP Model 3302A trigger/phase lock plug-in. For high speed (faster than 200 V/s) CV experiments, a Wavetec Model 143 20 MHz function generator and an EI-350 potentiostat built by R. Ensman of Ensman Instruments, Bloomington, IN, were used. Bulk electrolysis studies employed the PAR Model 173 together with a PAR Model 179 digital coulometer. Potentials were monitored using either a Keithley Model 178 or a HP 3435A digital multimeter.

Electrochemistry experiments employed a conventional three-electrode arrangement. The working electrode was either a platinum bead, a disk made of platinum, gold, or glassy carbon, or a hanging mercury drop electrode. An aqueous SCE was used as the experimental reference electrode at temperatures >273 K; a Ag/AgCl reference electrode was employed in experiments at lower temperatures. The reference electrode was always separated from the rest of the cell by a fine frit, and with the exception of coulometry experiments a Luggin probe was used in order to minimize *iR* loss. The electrode potentials were checked with ferrocene, used as an internal standard. All potentials reported in this paper are referenced to the ferrocene potential. Conversion to the SCE scale in THF requires addition of 0.56 V to the values quoted in this paper.

Electrode pretreatment procedures were as follows: platinum-bead electrodes were conditioned by holding the tip of the electrode in the vapors of refluxing nitric acid for 10 min followed by a cooling period to prevent cracking of the glass surrounding the electrode tip. The electrode was first rinsed with distilled water and then soaked in a solution of ferrous ammonium sulfate in 1 M sulfuric acid for an additional 10 min. It was then rinsed thoroughly with distilled water and dried with a tissue. The disk electrodes were cleaned by polishing with diamond pastes (Metadi II, from Buehler, Ltd.) of 6, 1, and then 0.25  $\mu$ m particle size, on an emery cloth. For ultramicroelectrodes, the polishing substance was Gamma Micropolish II, 0.05  $\mu$ m particle size, also from Buehler. After polishing, the electrode was washed with distilled water and wiped with a tissue.

Controlled-potential coulometry experiments were carried out in a Vacuum Atmospheres drybox under N<sub>2</sub>. The working electrode was either a platinum basket or a mercury pool. When the platinum basket was employed as the working electrode, a cocylindrical arrangement was used, whereby an

(9) Trogler, W. C. In *Organometallic Radical Processes*; Trogler, W. C., Ed.; Elsevier: Amsterdam, 1990; Chapter 9.

(10) Huang, Y.; Neto, C. C.; Pevear, K. A.; Banaszak Holl, M. M.; Schweigart, D. A.; Chung, Y. K. *Inorg. Chim. Acta* **1994**, *226*, 53.

(11) Donovan, B. T.; Geiger, W. E. *J. Am. Chem. Soc.* **1988**, *110*, 2335.

(12) Rausch, M. D.; Genetti, R. A. *J. Org. Chem.* **1970**, *35*, 3888.

(13) King, R. B. *Inorg. Chem.* **1966**, *5*, 82.

(14) Gilman, H.; Gaj, B. J. *J. Org. Chem.* **1957**, *22*, 447.

(15) Wakatsuki, Y.; Nomura, O.; Tone, H.; Yamazaki, H. *J. Chem. Soc., Perkin Trans. 2* **1980**, 1344.

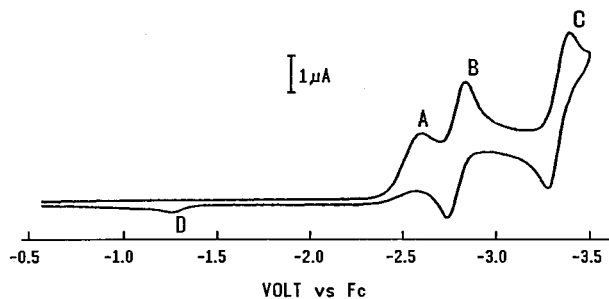


**Figure 1.** CV scan ( $\nu = 0.2 \text{ V s}^{-1}$ ) of  $5 \times 10^{-4} \text{ M}$  **1** in THF/0.1 M  $[\text{NBu}_4][\text{PF}_6]$  at 273 K at a Pt electrode.

auxiliary platinum electrode was placed inside a fine fritted compartment in order to separate the anodic and cathodic portions of the cell. For low-temperature experiments, the cell was submerged in a heptane bath which was cooled using a Flexible Temperature Systems (FTS) Flexi-Cool recirculating cooler.

Solvents employed in the electrochemistry experiments were dried and thoroughly degassed on a vacuum line prior to use. THF (Aldrich, Gold Label) was dried by refluxing for at least 8 h over potassium.

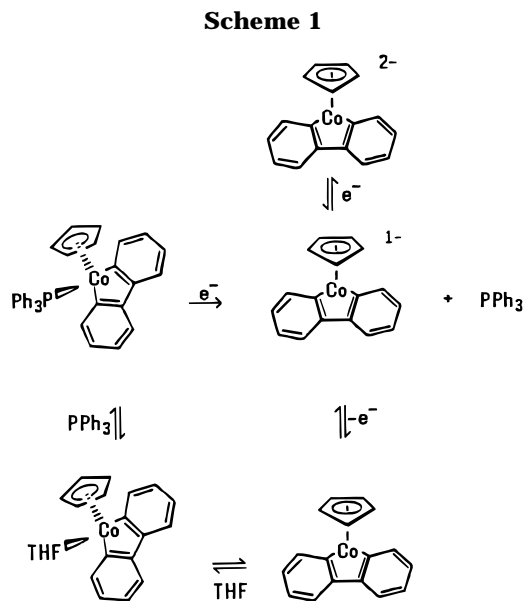
The supporting electrolytes  $[\text{NBu}_4][\text{PF}_6]$  and  $[\text{NBu}_4][\text{CF}_3\text{SO}_3]$ <sup>16</sup> were recrystallized from 95% ethanol and vacuum-dried at 373 K.

**Other Methods.** <sup>31</sup>P NMR spectra were recorded using a Bruker WM 250 MHz Spectrometer. <sup>1</sup>H NMR studies were carried out with a Bruker 270 MHz spectrometer. In the <sup>1</sup>H NMR experiments, solvent peaks were used to reference the chemical shifts relative to TMS. In <sup>31</sup>P NMR studies,  $\text{H}_3\text{PO}_4$  was used as an external standard. ESR spectra were obtained with a modified Varian E-4 spectrometer using DPPH as an external standard. Mass spectral analysis was performed on a Finnigan MAT 4500 series GC/MS system. Microanalysis was performed by Robertson Laboratory, Inc., Madison, NJ.

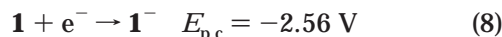
Extended Hückel MO calculations were performed with the CAChe suite of programs (CAChe Scientific Inc., Beaverton, OR) using the parameters collected by Alvarez.<sup>27</sup> Idealized bond lengths and bond angles were used for the  $\text{C}_5$  and  $\text{C}_6$  rings; the Co–C distances in the  $\text{CoC}_4$  ring were 1.934 Å, and the Co–Cp distance was 1.861 Å. The fluorenyl ring system defined the  $xz$  plane, and the Cp ring was parallel to the  $xy$  plane. Earlier calculations on cyclopentadienylcobaltacyclopentadiene,  $\text{CpCoC}_4\text{H}_4$ ,<sup>17</sup> showed an energy minimum for the metallacycle tilted 36° away from the Co–C vector (here taken as the  $z$  axis), 0.16 eV lower than the more symmetric structure. Accordingly, we extended our EHMO calculations to tilted conformations. For the cobaltfluorene, the minimum energy corresponded to the fluorenyl ring in the  $yz$  plane, increasing 0.72 eV for a 12° tilt and 4.47 eV for a 24° tilt. The additional delocalization afforded by the fluorenyl system is best exploited in the more symmetrical structure.

## Results and Discussion

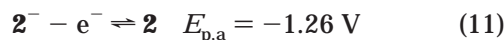
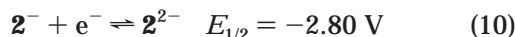
**Overview of Reductive Behavior of 1.** Cyclic voltammetry (CV) provides a simple map of the reduction of **1** and the consequent reaction products. Wave A of Figure 1 is the irreversible one-electron reduction of **1** ( $E_{p,c} = -2.56 \text{ V}$  at  $\nu = 0.2 \text{ V s}^{-1}$ ). Chemically reversible waves B and C arise from reduction of the two electrode products, namely the 17-electron metallacycle anion,  $\mathbf{2}^-$ , (B,  $E_{1/2} = -2.80 \text{ V}$ ) and free triphenylphosphine (C,  $E_{1/2}$



$= -3.34 \text{ V}$ ). The anodic wave D (which is enhanced when the negative-going scan is clipped after wave A) arises from the oxidation of  $\mathbf{2}^-$ . This scan and the experiments discussed below show that the reduction of **1** proceeds cleanly and rapidly through eqs 8 and 9 in an  $E_{\text{irrev}}C_{\text{rev}}$  mechanism.



We will also show that  $\mathbf{2}^-$  may be reduced to the corresponding 18-electron dianion,  $\mathbf{2}^{2-}$ , through eq 10 (wave B) or oxidized to the 16-electron metallacycle, **2** (eq 11, wave D). The latter immediately coordinates available two-electron donors, L (eq 12), to regenerate a neutral, 18-electron, metallacycle. If  $L = \text{PPh}_3$ , the product  $\mathbf{2}\text{-L}$  of eq 12 is simply the starting material **1**. Other possibilities such as  $L = \text{THF}$  or  $\text{P}(\text{OMe})_3$  will also be discussed.



The overall reaction mechanism is indicated in Scheme 1, wherein formation of **2** is assumed to lead first to a THF adduct owing to the large excess of THF over  $\text{PPh}_3$ . Replacement of THF by the phosphine ligand would eventually follow.

**Formation of the 17-Electron Anion  $\mathbf{2}^-$ .** The diffusion-controlled<sup>18</sup> one-electron<sup>19</sup> reduction wave (A) of **1** has a peak breadth ( $E_p - E_{p/2}$ ) of 90 mV, consistent with an irreversible electron transfer having  $\alpha n =$

(18) A description of the voltammetric diagnostics may be found in: Geiger, W. E. In *Electroanalytical Chemistry*; Kissinger, P., Heinemann, W., Eds.; Marcel Dekker: New York, 1996; pp 683 ff.

(19) The reduction wave height was approximately equal to the one-electron height of decamethylferrocene. More definitively, it was about three-fourths the height of the reversible one-electron oxidation wave of **2** to  $\mathbf{2}^+$ , consistent with a one-electron irreversible reduction having an  $\alpha$  value of 0.5, both measurements being made at 253 K. The oxidation of **2** to  $\mathbf{2}^+$  was reversible by cyclic voltammetry,  $E_{1/2} = 0.31 \text{ V}$  in THF; bulk oxidation at 218 K produced a stable monocation.

(16) Rousseau, K.; Farrington, G. C.; Dolphin, D. *J. Org. Chem.* **1972**, *37*, 3971.

(17) Wakatsui, Y.; Nomura, O.; Kitaura, K.; Morokuma, K.; Yamazaki, H. *J. Am. Chem. Soc.* **1983**, *105*, 1970.



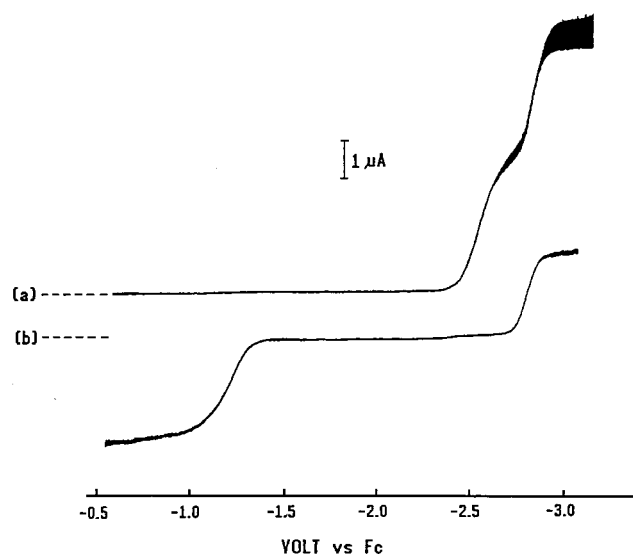


**Figure 2.** Steady-state voltammograms at the rotating Pt electrode recorded (a) before and (b) after bulk reduction of  $5 \times 10^{-4}$  M **1** in THF/0.1 M [NBu<sub>4</sub>][PF<sub>6</sub>] at  $E_{\text{appl}} = -2.56$  V (scan rate  $5 \text{ mV s}^{-1}$ ,  $T = 273$  K). The dotted line gives zero current.

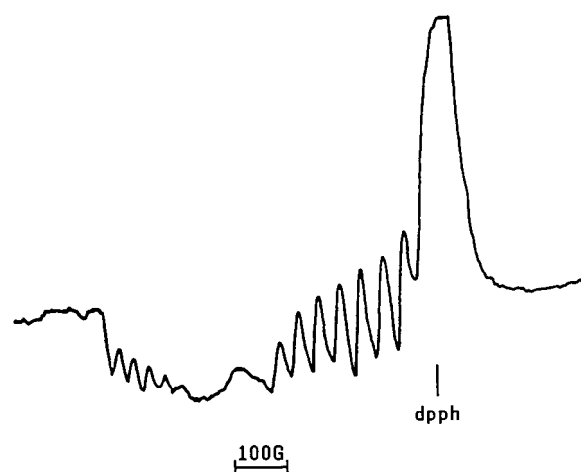


**Figure 3.** EPR spectrum of a frozen solution ( $T = 196$  K) of **2**<sup>-</sup> in THF/0.1 M [NBu<sub>4</sub>][PF<sub>6</sub>]. The sample was taken from a  $5 \times 10^{-4}$  M solution of **1** which had been electrolyzed at  $E_{\text{appl}} = -2.56$  V.

0.52.<sup>20</sup> No coupled anodic return feature was observed even at scan rates of 5000 V/s at a  $10 \mu\text{m}$  diameter Pt electrode, placing an upper limit on the lifetime of 19-electron **1**<sup>-</sup> at about  $40 \mu\text{s}$  at 298 K. CV at 213 K ( $v = 0.2 \text{ V s}^{-1}$ ) also showed no reversibility for wave A.

Compound **1** was exhaustively electrolyzed at 273 K with  $E_{\text{appl}} = -2.56$  V, resulting in a color change from yellow to orange and a coulomb count of 1.1 faraday/equiv. A comparison of steady-state voltammograms (Figure 2) demonstrates that after bulk electrolysis waves B and D are present as cathodic and anodic features, respectively, replacing the cathodic wave of **1**. A sample of this electrolyzed solution taken for ESR analysis gave an intense signal as a frozen solution (Figure 3) which consisted of two resolved octets (hyperfine splitting to <sup>59</sup>Co,  $I = 7/2$ ) and a broad singlet

(20) The peak breadth,  $E_p - E_{p/2}$ , is  $48 \text{ mV}/\alpha n$  for an electrochemically irreversible wave, where  $\alpha$  is the electrochemical transfer coefficient.

corresponding to the three principal components of the **g** matrix. The spacing of the hyperfine features is as expected from a second-order perturbation theory of the simple spin Hamiltonian containing electronic Zeeman and electron–nuclear hyperfine interaction terms with coincident principal axes for the **g** and hyperfine matrices. The coincidence of the principal axes suggests a model with  $C_{2v}$  or higher symmetry, consistent with the conclusions based on EHMO calculations.

The spectrum was interpreted by simulations (see Supporting Information) to give  $g_1 = 2.330$ ,  $g_2 = 2.107$ ,  $g_3 = 1.996$ ,  $A_1 = 36.8 \times 10^{-4} \text{ cm}^{-1}$ ,  $A_2 = 39.9 \times 10^{-4} \text{ cm}^{-1}$ , and  $A_3 < 10 \times 10^{-4} \text{ cm}^{-1}$ . If the metal contribution to the SOMO is a single 3d orbital, we expect the hyperfine splittings to be given by

$$A_{\parallel} = \langle A \rangle - (4/7)P\rho_d \quad (13)$$

$$A_{\perp} = \langle A \rangle + (2/7)P\rho_d \quad (14)$$

where  $P = 282 \times 10^{-4} \text{ cm}^{-1}$  and  $\rho_d$  is the 3d spin density.<sup>21</sup> With  $A_{\parallel} = [0(\pm 10)] \times 10^{-4} \text{ cm}^{-1}$  and  $A_{\perp} = [38.4(\pm 1.5)] \times 10^{-4} \text{ cm}^{-1}$ , we have  $A_{\parallel} - A_{\perp} = [38.4(\pm 1.5)] \times 10^{-4} \text{ cm}^{-1}$ , and  $\rho_d = 0.16 \pm 0.04$ . Given the substantial *g* value anisotropy, there is almost certainly a sizable spin–orbit coupling correction which should be applied, but with a highly delocalized system, such a correction cannot be made using the *g* components alone. Nonetheless, it is clear that the SOMO is extensively delocalized over the carbocyclic fragments with only a modest contribution from the metal. This conclusion is entirely consistent with the EHMO calculations, which predict that the singly occupied molecular orbital (SOMO) has contributions from Co 3d<sub>yz</sub> (27.4%) and 4p<sub>y</sub> (4.2%), from Cp C 2p<sub>z</sub> (59.6%), and from the fluorenyl C 2p<sub>z</sub> (7.6%). The relatively large magnetogyric ratio of cobalt produces not only large hyperfine splittings but also relatively large spectral line widths when the anisotropies of those splittings are taken into account. This is undoubtedly why proton splittings from the Cp ring are not resolved in spectra of **2**<sup>-</sup>.

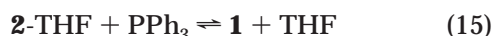
By observing the decay of wave D with time after the completion of the bulk electrolysis it was determined that the half-life of the 17-electron metallacycle **2**<sup>-</sup> was about 1 h at room temperature. Wave D was ultimately replaced by a new (irreversible) anodic wave at  $E_{p,a} = -1.14$  V of unidentified origin.

**Confirmation of Liberation of PPh<sub>3</sub> in Reduction of **1**.** The postulate that rapid ejection of triphenylphosphine (eq 9) follows formation (eq 8) of the 19-electron metallacycle **1**<sup>-</sup> was confirmed by experiments addressing both the CV and electrolytic time scales. Regarding the former, the reversible reduction of the product wave (C) at  $E_{1/2} = -3.34$  V was assigned to free PPh<sub>3</sub> on the basis of its potential matching that of PPh<sub>3</sub> in a control experiment. Addition of a 10-fold excess of PPh<sub>3</sub> to a solution of **1** resulted in a proportional increase of the current for wave C, but no changes in the other waves were observed. Regarding the synthetic time scale, a solution of **1** in *d*<sub>8</sub>-THF was sealed under vacuum in an NMR tube which contained a sidearm with a vacuum-deposited potassium mirror. The solution was allowed contact with the mirror and then poured into the tube and monitored by <sup>31</sup>P{<sup>1</sup>H}

(21) Morton, J. R.; Preston, K. F. *J. Magn. Reson.* **1978**, *30*, 577.

spectroscopy. A multiplet present prior to reduction at 63 ppm was replaced by a singlet at  $-4.8$  ppm for free  $\text{PPh}_3$ .

**Formation and Fate of 16-Electron  $\mathbf{2}$ .** The oxidation of  $\mathbf{2}^-$  in wave D produces 16-electron  $\mathbf{2}$ , which, as a coordinatively-unsaturated molecule, is expected to coordinate Lewis bases that might be present. Interestingly, CV scans reversed after transversal through the oxidation wave D did not reveal the presence of wave A in the negative-going branch. This means that  $\mathbf{2}$  did not re-form  $\mathbf{1}$  through eq 12, i.e., by recoordination of  $\text{PPh}_3$ , at least on the CV time scale. The original compound  $\mathbf{1}$  was re-formed, however, in 65% yield when the oxidation of wave D was accomplished in a bulk electrolysis. These facts imply that the 16-electron complex  $\mathbf{2}$  reacts rapidly to give an intermediate which slowly coordinates  $\text{PPh}_3$  to re-form  $\mathbf{1}$  (eq 15). Given the makeup of the



electrolyte solution, the intermediate is almost certainly the solvent adduct  $\mathbf{2}\text{-THF}$ . Despite the much lower basicity of THF compared to a phosphine, the concentration ratio of about  $10^4$  THF/ $\text{PPh}_3$  undoubtedly makes the THF adduct the kinetic product in the oxidation of  $\mathbf{2}^-$ . Experiments in which a 10-fold excess of  $\text{PPh}_3$  was present in solution gave the following results: CV, still no evidence of wave A after scanning through wave D; bulk re-electrolysis, 75% re-formation of  $\mathbf{1}$ . The overall reduction and reoxidation of  $\mathbf{1}$  is therefore seen to be chemically reversible; mechanistically speaking, however, the process occurs through two electrochemically irreversible processes (eqs 8 and 9 for reduction; eqs 11 and 12 ( $L = \text{THF}$ ) and 15 for reoxidation) in an EC/ECC sequence.

**Formation of the 18-Electron Metallacyclic Dianion  $\mathbf{2}^{2-}$ .** The existence and possible persistence of the 18-electron complex  $\mathbf{2}^{2-}$  suggested by the reversibility of wave B was explored. Generated through bulk electrolysis, the dianion decayed to unknown products. It was successfully produced, however, through alkali-metal reductions of either  $\mathbf{1}$  or the trimethyl phosphite complex  $\mathbf{3}$ . The  $^1\text{H}$  NMR spectra generated from reduction of  $\mathbf{3}$  by a K mirror were more readily interpreted owing to lack of interference from the reduction products of  $\text{PPh}_3$ , so we now turn to that data.

When the  $\text{P}(\text{OMe})_3$  adduct  $\mathbf{3}$  underwent prolonged contact with a potassium mirror in  $d_8\text{-THF}$  under a sealed vacuum, the  $^1\text{H}$  NMR spectrum of  $\mathbf{3}$  was replaced by one assigned to  $\mathbf{2}^{2-}$  (Figure 4). Assignments made on the basis of decoupling and NOE experiments (described in detail in Supporting Information) are given in Table 2 for  $\mathbf{3}$  and  $\mathbf{2}^{2-}$ . As expected for a complex of increased negative charge, significant increases in shielding are seen for almost all the protons in the fluorenyl ring of  $\mathbf{2}^{2-}$ . An exception is proton 1, shifted to 8.28 ppm in  $\mathbf{2}^{2-}$  from 7.64 ppm in  $\mathbf{3}$ . This position is likely to be dominated by the anisotropy of the Cp ring, leading to a net deshielding of this proton. These data confirm that charge is delocalized into the fluorenyl ring in  $\mathbf{2}^{2-}$  with the position farthest from the metal (proton 4) having the smallest charge increase. The largest increase in shielding, however, is associated with the Cp ring, for which the chemical shift increases by 0.75 ppm. This is consistent with the MO calculations (see

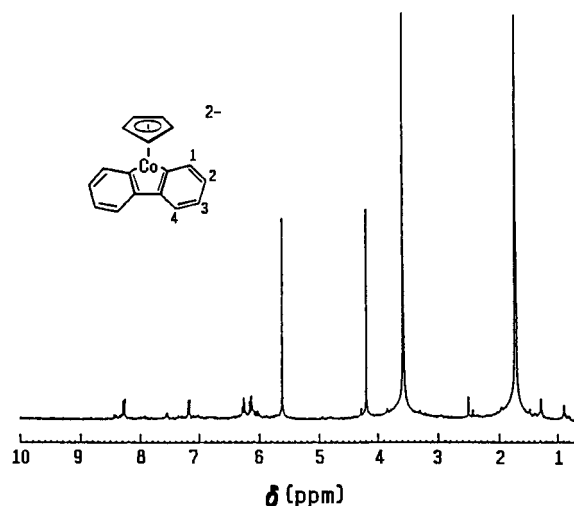


**Figure 4.**  $^1\text{H}$  NMR spectrum of  $\mathbf{2}^{2-}$  obtained after reduction of  $\mathbf{3}$  in  $d_8\text{-THF}$  with potassium mirror.

**Table 1. Formal Potentials vs Ferrocene of Cobaltacycles in THF/0.1 M  $[\text{NBu}_4][\text{PF}_6]$  at Ambient Temperature**

compd	process	couple	potential, V
$\text{Cp}(\text{PPh}_3)\text{CoC}_{12}\text{H}_8$ ( $\mathbf{1}$ )	redn	0/1-	-2.56 (irrev, $E_{p,c}$ )
$\mathbf{1}$	oxdn	0/1+	0.31 <sup>a</sup>
$[\text{CpCoC}_{12}\text{H}_8]^{2-}$ ( $\mathbf{2}^-$ )	redn	1-/2-	-2.80
$\mathbf{2}^-$	oxdn	1-/0	-1.26 (irrev, $E_{p,a}$ )
$\text{Cp}[\text{P}(\text{OMe})_3]\text{CoC}_{12}\text{H}_8$ ( $\mathbf{3}$ )	redn	0/1-	-2.76 (irrev, $E_{p,c}$ )
$\mathbf{3}$	oxdn	0/1+	0.42 <sup>b</sup>
$\text{Cp}(\text{PEt}_3)\text{CoC}_{12}\text{H}_8$	oxdn	0/1+	0.26

<sup>a</sup> Chemically irreversible at 298 K ( $v = 0.2$  V/s), increasingly reversible at lower temperatures, and finally fully reversible at 253 K (using  $[\text{NBu}_4][\text{CF}_3\text{SO}_3]$  as supporting electrolyte). <sup>b</sup> Limited chemical reversibility at  $v = 0.2$  V/s.

**Table 2. Comparison of  $^1\text{H}$  Chemical Shifts for  $\text{Cp}[\text{P}(\text{OMe})_3]\text{CoC}_{12}\text{H}_8$  ( $\mathbf{3}$ ) and  $[\text{CpCoC}_{12}\text{H}_8]^{2-}$  ( $\mathbf{2}^{2-}$ ) in  $d_8\text{-THF}$  (Values in ppm Relative to TMS)**

proton	$\delta(\mathbf{3})$	$\delta(\mathbf{2}^{2-})$	$\delta(\mathbf{3}) - \delta(\mathbf{2}^{2-})$
1	7.64	8.28	-0.64
2	6.71	6.15	0.56
3	6.87	6.27	0.60
4	7.37	7.18	0.19
Cp	4.94	4.19	0.75

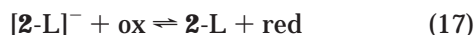
above), which indicate a greater involvement of the Cp ring than the fluorenyl framework in the redox anion(s). The dianion retains at least  $C_s$  symmetry, a conclusion also consistent with the interpretation of the ESR spectrum of the 17-electron anion.

**Reaction of  $\mathbf{2}^-$  with  $\text{P}(\text{OMe})_3$ .** Complex  $\mathbf{1}$  undergoes electrocatalytic substitution reactions when it is reduced in the presence of phosphines or phosphites that are more basic than  $\text{PPh}_3$ . This implies that the  $17 e^-/19 e^-$  equilibrium of eq 16 is indeed reversible, even though



it may lie far to the left. To complete the electrocatalytic cycle, the  $19 e^-$  adduct  $[\mathbf{2}\text{-L}]^-$  must be oxidized to the

18-electron complex **2-L** by either the electrode or by a homogeneous oxidant (eq 17). We show below that the



homogeneous reaction route dominates under most conditions. Preceding that discussion, however, we briefly describe the electrochemical behavior of the trimethyl phosphite complex **3**, which is formed in the cathodically initiated ETC substitution reaction of **1** in the presence of  $\text{P}(\text{OMe})_3$ .

CV scans of **3** obtained under the same conditions as described in Figure 1 revealed a reductive mechanism the same as that observed for **1**. The reduction of **3** is more negative ( $E_{p,c} = -2.80$  V) than that of **1**, but the other CV features (waves C and D) are identical. Bulk reduction of **3** (1 faraday/equiv) gave the expected solution of  $\mathbf{2}^-$  resulting from ejection of  $\text{P}(\text{OMe})_3$  from  $\mathbf{3}^-$ .

### Electrocatalytic Substitution Reactions of **1**.

When **1** is reduced in the presence of more nucleophilic phosphines or phosphites (L), substitution products (L for  $\text{PPh}_3$ ) are observed; the substitution reaction is electrocatalytic with an efficiency that depends on the concentration of the reactant **1**. These experiments give strong confirmation of the importance of 17  $e^-$ /19  $e^-$  equilibria (eq 16) in the substitution reactions.

Complex **1** is unchanged for several hours in the presence of a 10-fold excess of  $\text{P}(\text{OMe})_3$ . Electrolysis of the mixture at  $-2.56$  V gives  $\mathbf{2}^-$  (Figure 5b, anodic wave at  $-1.26$  V, ca. 75% yield)<sup>22</sup> and cathodic features at ca.  $-2.80$  V identical with those of the trimethyl phosphite complex **3** (25% yield). The catalytic efficiency was low, about 1.2, as implied by the coulomb count,  $n_{\text{app}} = 0.83$ . Replicating the experiment at higher concentrations of  $\text{P}(\text{OMe})_3$ , but keeping the concentration of **1** at 0.5 mM, did not increase the efficiency of the electrocatalysis (Table 3). Scheme 2 accounts for this inefficiency. In it, the 17-electron metallacycle  $\mathbf{2}^-$  is seen to be in equilibrium with three possible 19-electron anions:  $[\mathbf{2-THF}]^-$ ,  $[\mathbf{2-PPh}_3]^-$ , and  $[\mathbf{2-P}(\text{OMe})_3]^-$ . The oxidation of  $[\mathbf{2-P}(\text{OMe})_3]^-$  required to form the neutral substitution product **3** may occur either at the electrode ( $E_{\text{appl}} = -2.56$  V is sufficient to reoxidize  $[\mathbf{2-P}(\text{OMe})_3]^-$  but not  $[\mathbf{2-PPh}_3]^-$ ) or in homogeneous solution. Any homogeneous oxidation of  $[\mathbf{2-PPh}_3]^-$ , re-forming **1**, leads to no net chemical change through this branch of Scheme 2 as long as the applied potential remains sufficiently negative to reduce any **1** that is formed.

If the solution containing  $\mathbf{2}^-$  and the two competing Lewis bases is exposed to a Pt-gauze electrode with a potential sufficient to oxidize  $\mathbf{2}^-$  (e.g.,  $E_{\text{appl}} = -1.05$  V) in a "reverse electrolysis", then the yield of **3** rises dramatically. Figure 5 shows the voltammograms obtained in such an experiment. The top two scans were recorded after the cathodic electrolysis of **1** in the presence of a 20-fold excess of  $\text{P}(\text{OMe})_3$ ; the cathodic wave at  $E_{1/2}$  ca.  $-2.8$  V arises from the reduction of **3**, whereas the anodic wave at  $-1.2$  V is from  $\mathbf{2}^-$ . No unreacted **1** is detected. The bottom two scans were recorded after reverse electrolysis at  $E_{\text{appl}} = -0.9$  V and

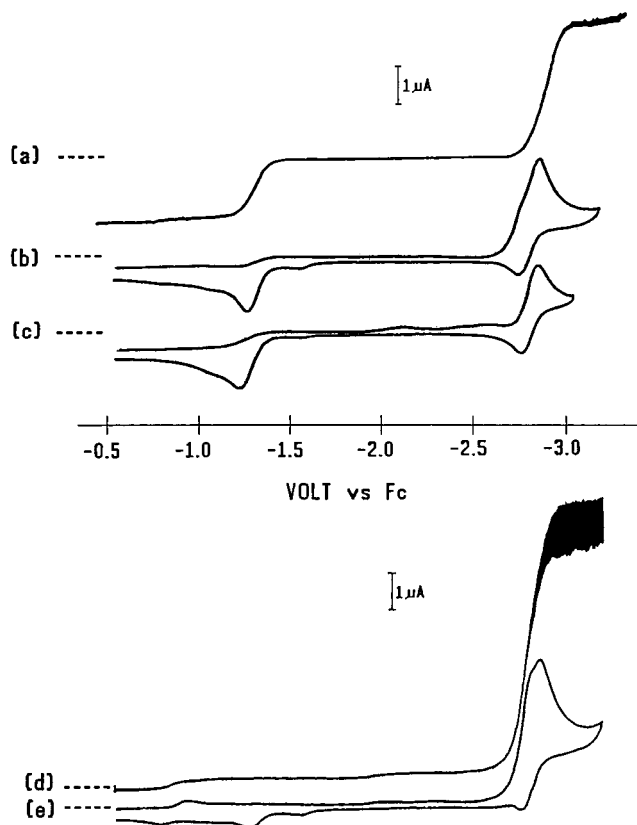


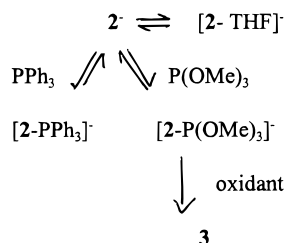
**Figure 5.** (top) Scans after bulk reduction of  $5 \times 10^{-4}$  M **1** at  $E_{\text{appl}} = -2.56$  V in THF: (c) CV scan ( $v = 0.2$  V  $s^{-1}$ ) of pure **1** with no  $\text{P}(\text{OMe})_3$  present; (a,b) RPE and CV scans after electrolysis in the presence of  $1 \times 10^{-2}$  M  $\text{P}(\text{OMe})_3$ . (bottom) RPE (d) and CV (e) scans after "reverse electrolysis", i.e., back oxidation of  $\mathbf{2}^-$  at  $E_{\text{appl}} = -0.9$  V in the presence of a 20-fold excess of  $\text{P}(\text{OMe})_3$  showing virtually exclusive formation of **3**.

**Table 3. Efficiencies of Electrocatalytic Substitution of  $\text{PPh}_3$  by  $\text{P}(\text{OMe})_3$  through Bulk Cathodic Reduction of **1** in the Presence of  $\text{P}(\text{OMe})_3$  in THF at Ambient Temperatures**

concn of <b>1</b> (mM)	concn of $\text{P}(\text{OMe})_3$ (mM)	coulomb count, faraday/equiv <sup>a</sup>	chain efficiency
0.5	10	0.83	1.25
0.5	52	0.91	1.10
4.6	4.6	0.37	2.70
4.6	456	0.10	10.0

<sup>a</sup> Ratio of coulombs per equivalent of **1** required to achieve >95% conversion to **3**.

### Scheme 2



show that **3** is almost the exclusive product when  $\mathbf{2}^-$  is oxidized in the presence of excess  $\text{P}(\text{OMe})_3$ .

That the required oxidation step can also be accomplished with a chemical oxidant is implied when considering that the catalytic efficiency of the substitu-

(22) The use of observed currents to calculate "percent yields" of the electrochemical reactions assumes similar diffusion coefficients for reactants and products.



tion reaction rose by an order of magnitude when more concentrated solutions of **1** were employed (Table 3). In these experiments the reactant **1** acts as the oxidant in Scheme 2 and in so doing converts another mole of reactant to the unsaturated intermediate  $2^-$  required for the substitution. The potentials involved suggest that **1** can reduce 19-electron  $[2-L]^-$  but not 17-electron  $2^-$ . The feasibility of **1** acting as an oxidant was proven by adding 0.2 equiv of **1** at open circuit to an electrolyzed solution containing  $2^-$  and 10 equiv of  $P(OMe)_3$ . After about 20 min the current due to  $2^-$  had decreased and that due to **3** had increased, both by about one-third. After 0.8 equiv of **1** was added and the mixture was stirred for 2 h, the yield of **3** doubled and there was no voltammetric evidence of **1**.

The oxidation chemistry can also be performed by an oxidant unrelated to those appearing in the 17  $e^-$ /19  $e^-$  equilibria. This was demonstrated using 9-fluorenone (FL), which is reduced at  $E_{1/2} = -1.88$  V to a radical anion. Although FL is a very weak oxidizing agent, it is capable of oxidizing the 19-electron systems  $[2-L]^-$  of Scheme 2. FL was added at open circuit to a solution containing  $2^-$  and excess  $P(OMe)_3$ . After addition of 0.21 equiv of FL the amount of **3** increased at the expense of  $2^-$  and the voltammetric wave for FL at  $E_{1/2} = -1.88$  V was completely anodic, indicating that the fluorenone was present in the reduced form as  $[FL]^-$ . This trend continued as more FL was added until all the  $2^-$  had reacted. Further addition of FL gave a cathodic contribution for the fluorenone wave, signaling the end of the "redox titration" and the absence of any 17  $e^-$  cobalt cycle.

### Conclusions

Reductively induced ETC reactions with high turnover numbers are thought to require an intermediate which has (i) coordinative unsaturation and (ii) at least a modest ability to coordinate an incoming nucleophile. In polynuclear complexes, cleavage of metal-metal or metal-ligand bonds may generate the required 17-electron center. In such systems the distribution of charge over several metal centers apparently favors the coordination of the nucleophile and these ETC reactions tend to be quite efficient.<sup>23</sup> Although some mononuclear-

based ETC reactions may also be rapid and efficient,<sup>24</sup> other cases of very slow catalysis are known.<sup>25</sup> It seems clear that the equilibrium constant and kinetics of the 17-electron/19-electron equilibrium are the key factors in determining which of these scenarios is followed.

Our studies of the cobaltacyclic system allow some insights to be gained regarding the properties of a 17-electron mononuclear intermediate and its role in ETC processes. The property of the intermediate  $2^-$  responsible for our ability to monitor it, namely its kinetic and thermodynamic stability, is also responsible for its inefficiency as a propagating agent in the electron-transfer chain. One aspect of this stability is seen in the apparent positions of the equilibria of Scheme 2, which must strongly disfavor both the phosphine and phosphite adducts. In the present system the 17-electron anion  $2^-$  constitutes a "resting state" in the propagation sequence and a productive exit from this state (i.e., one which produces **3**) depends on the presence of an oxidant. The stability of  $2^-$  may be attributed in part to its ability to weakly coordinate a THF molecule (Scheme 2), a property arising from the low (ca. 30%) metallic character of the SOMO in the formal 17-electron anion. Our results stand in contrast to another 17  $e^-$ /19  $e^-$  system involving the ETC substitution of  $PPh_3$  for  $I^-$  in  $CpFe(CO)_2I$ .<sup>26</sup> In the iron system a set of competitive equilibria are involved which are analogous to those of Scheme 2, but the 17  $e^-$  complex (the Fp radical) is unstable, subject to rapid dimerization to form  $[Cp_2Fe(CO)_2]_2$ , precluding the solution characterization of the reactive intermediate. The comparatively greater stability of  $2^-$ , while allowing for fuller characterization of the intermediate, is accompanied by a lower electrophilicity which lowers the efficiency of the ETC process.

**Acknowledgment.** We are grateful to the National Science Foundation for support of this work.

**Supporting Information Available:** The NOE spectrum of  $2^{2-}$  and discussion of assignments and simulation of frozen ESR spectrum of  $2^-$ . This material is available free of charge via the Internet at <http://pubs.acs.org>.

OM990246G

(23) (a) Hinkelman, K.; Mahlendorf, F.; Heinze, J.; Schacht, H.-T.; Field, J. S.; Vahrenkamp, H. *Angew. Chem., Int. Ed. Engl.* **1987**, *26*, 352. (b) Arewgoda, M.; Rieger, P. H.; Robinson, B. H.; Simpson, J.; Visco, S. J. *J. Am. Chem. Soc.* **1982**, *104*, 5633. (c) Holzmeier, P.; Kisch, H.; Kochi, J. K. *J. Organomet. Chem.* **1990**, *382*, 129. (d) Fassler, T.; Huttner, G.; Gruenauer, D.; Fiedler, S.; Eber, B. *J. Organomet. Chem.* **1990**, *381*, 409.

(24) (a) Neto, C. C.; Kim, S.; Meng, Q.; Sweigart, D. A.; Chung, Y. K. *J. Am. Chem. Soc.* **1993**, *115*, 2077. (b) Huang, Y.; Neto, C. C.; Pevear, K. A.; Banaszak Holl, M. M.; Sweigart, D. A.; Chung, Y. K. *Inorg. Chim. Acta* **1994**, *226*, 53.

(25) (a) Miholova, D.; Vlcek, A. A. *J. Organomet. Chem.* **1985**, *279*, 317. (b) Olbrich-Deussner, B.; Kaim, W. *J. Organomet. Chem.* **1988**, *340*, 71.

(26) Liu, Z.; Gipson, S. L. *J. Organomet. Chem.* **1998**, *553*, 269.

(27) Alvarez, S. *Tables of Parameters for Extended Hückel Calculations*; University of Barcelona: Barcelona, Spain, 1989.